Eur Biophys J (1998) 27: 455–465

ARTICLE

A. Marx · M. Thormählen · J. Müller · S. Sack
E.-M. Mandelkow · E. Mandelkow

Conformations of kinesin: solution vs. crystal structures and interactions with microtubules

Received: 30 January 1998 / Revised version: 6 April 1998 / Accepted: 9 April 1998

Abstract Recently, the molecular structures of monomeric and dimeric kinesin constructs in complex with ADP have been determined by X-ray crystallography (Kull et al. 1996; Kozielski et al. 1997a; Sack et al. 1997). The "motor" or "head" domains have almost identical conformations in the known crystal structures, yet the kinesin dimer is asymmetric: the orientation of the two heads relative to the coiled-coil formed by their neck regions is different. We used small angle solution scattering of kinesin constructs and microtubules decorated with kinesin in order to find out whether these crystal structures are of relevance for kinesin's structure under natural conditions and for its interaction with microtubules. Our preliminary results indicate that the crystal structures of monomeric and dimeric kinesin are similar to their structures in solution, though in solution the center-of-mass distance between the motor domains of the dimer could be slightly greater. The crystal structure of dimeric kinesin can be interpreted as representing two equivalent conformations. Transitions between these or very similar conformational states may occur in solution. Binding of kinesin to microtubules has conformational effects on both, the kinesin and the microtubule. Solution scattering of kinesin decorated microtubules reveals a peak in intensity that is characteristic for the B-surface lattice and that can be used to monitor the axial repeat of the microtubules under various conditions. In decoration experiments, dimeric kinesin dissociates, at least partly, leading to a stoichiometry of 1:1 (one kinesin head per tubulin dimer; Thormählen et al. 1998a) in contrast to the stoichiometry of 2:1 reported for dimeric ncd. This discrepancy is possibly due to the effect of steric hindrance between kinesin dimers on adjacent binding sites.

Key words Microtubules · Motor proteins · Kinesin · X-ray crystallography · Small angle X-ray scattering · Cell motility

A. Marx (✉) · M. Thormählen · J. Müller · S. Sack
E.-M. Mandelkow · E. Mandelkow
Max-Planck-Unit for Structural Molecular Biology,
c/o DESY, Notkestrasse 85, D-22607 Hamburg, Germany

Introduction

Kinesin is the founding member of a family of motor proteins that transport membrane bounded organelles along microtubules. The conventional kinesin is a heterotetramer, consisting of two heavy chains and two light chains. The heavy chain comprises three major domains: a motor or head domain that is responsible for nucleotide binding and hydrolysis as well as for interaction with microtubules, a tail domain that binds to the light chains which are believed to be important for specificity in cargo binding, and a stalk domain that forms a coiled coil with the stalk of the second heavy chain and serves as a flexible link between the motor and the cargo. Most members of the kinesin family are twin motors and move toward the plus end of the microtubule, as is the case for conventional kinesin. However, there exist also kinesin related proteins that have only one motor domain, or that differ from conventional kinesin by moving in the opposite direction, to the minus end, like ncd (for review see Brady 1995; Cole and Scholey 1995; Hirokawa 1996; Vale and Fletterick 1997).

From kinetic measurements of ATP hydrolysis and phosphate release induced by microtubule interaction it has been concluded that both heads of dimeric kinesin work cooperatively and processively (Ma and Taylor 1997; Jiang et al. 1997; Gilbert et al. 1998). This suggests a "hand-over-hand" mechanism (Cross 1997). It is not yet clear, however, whether processivity and cooperativity are essential for kinesin's motility. Alternatively, these properties could be special to conventional kinesin, improving its efficiency but not excluding other motors, especially the monomeric kinesins, to move slowly without showing processivity and cooperativity.

The molecular structures of the kinesin (Kull et al. 1996) and the ncd (Sablin et al. 1996) motor domains revealed an unexpected similarity to myosin, the paradigm of a motor protein that moves along actin filaments. For myosin, a "lever arm" movement of the stalk domain induced by hydrolysis of ATP to ADP has been proposed (Holmes 1997). Although the kinesin and ncd structures did not in-

clude the stalk domain, it was tempting to speculate that the microtubule motors use a similar mechanism to convert the energy stored in ATP into mechanical work (Rayment 1996; Vale 1996). By using longer constructs of the kinesin motor domain including the initial part of the stalk domain (hereafter called the "neck", as it connects the head with the stalk of the molecule) it became evident, that the relative orientation of head and stalk in kinesin is quite different from that in myosin (Sack et al. 1997; Kozielski et al. 1997a). This implies that the mechanisms of these motor proteins are not strictly comparable.

In the following we first summarize the findings on the crystal structure of monomeric and dimeric kinesin constructs, both including the head domain and different lengths of the neck domain. Implications for kinesin's mechanism of force generation and transduction depend on how strongly the conformation in the crystal structure is determined by intrinsic properties of the molecule or by crystal contacts. To address this question, complementary results from small angle solution scattering of kinesin and of kinesin decorated microtubules are considered. Finally we combine the crystal structure with results from electron microscopy and image reconstruction.

Materials and methods

Recombinant kinesin constructs were expressed in *Escherichia coli* and purified from cell lysates as described (Thormählen et al. 1998a) by one of the following methods: sK395 and sK498 were purified by microtubule affinity binding and sedimentation; sK338 was purified by Ni-NTA affinity chromatography (Kozielski 1997); rK354 and rK379 were purified by chromatography on P11-phosphocellulose followed by Mono Q column chromatography.

Tubulin was prepared by phosphocellulose (PC) chromatography as described by Mandelkow et al. (1985). Microtubules were polymerized from solutions containing 10–15 mg/ml of PC-tubulin by incubation at 37 °C for 20 min. In some preparations taxol was added at 50 μM, either before or after polymerization. Decoration of microtubules with kinesin constructs was performed by adding 3 moles of kinesin construct per mole of tubulin dimer in the presence of 1 mM AMP-PNP. After incubation for 5 min at room temperature decorated microtubules were sedimented by centrifugation and unbound kinesin was removed with the supernatant. Gels of microtubules with uniaxial orientation distribution were prepared by extrusion of pellets obtained by centrifugation into a 0.7 mm diameter, fused silica capillary, inducing a partial orientation of the microtubules parallel to the capillary.

Crystals of rK379 were grown as described by Kozielski et al. (1997b). A data set was collected at the EMBL/ESRF synchrotron beamline BM14 (Grenoble, France) with resolution up to 2.8 Å. The data were processed using DENZO and SCALEPACK (Otwinowski and Minor 1997), resulting in a data set that was complete up to 3.0 Å (97.7% overall completeness, $I/\sigma > 2$ for 80.0% in resolution shell 3.10-3.02 Å, for 62.0% in the highest resolution shell, 2.86-2.80 Å). Using this data set the structure of rK379, which was previously solved by MIR (Kozielski et al. 1997a), was re-determined independently by molecular replacement, using the head domain of monomeric rK354 (Sack et al. 1997) as a starting model. Programs of the CCP4 suite (Collaborative Computing Project No. 4, 1994) were used during further data processing and model refinement. Analysis of the combined rotational-translational correlation of two head domains by AMoRe (Navazza 1994) lead unambiguously to a single solution. The initial model (R-factor 41.4%) was completed and refined by several rounds using Turbo-Frodo (Cambillau et al. 1996) for rebuilding the model and Refmac (Murshudov et al. 1996) for maximum likelihood refinement. In order to reduce bias possibly introduced by the start model the structure was subjected to simulated annealing by XPLOR (Brünger 1992) at an intermediate stage of the refinement. At present the model contains amino acids 2-237 and 258-370 of both protein chains, as well as two ADP molecules. The R-factor is 26.2%, with an R-free value of 36.2% (resolution range 15-2.8 Å). Further refinement is in progress.

Small angle X-ray scattering experiments were performed on instrument X33 of the EMBL Outstation at DESY, Hamburg (Koch and Bordas 1983). Scattering intensities were recorded by using a quadrant detector for azimuthal integration or a linear detector aligned parallel to the direction of preferential orientation in the case of stretched specimen. Bragg spacings $s = 2 \sin \theta/\lambda$, with 2θ scattering angle, λ wavelength, were calibrated by the reflections of collagen fibrils from turkey tendon assuming a repeat of 64 nm. The absolute accuracy of *s*-values depends on the accuracy of the standard used for calibration (<2%). Detection of small changes of spatial periodicities with time or between different preparations requires a high reproducibility of *s*-measurements. This depends on the stability of the experimental setup and the beam position over the time between different measurements. Corresponding uncertainties of *s*-values are considerably smaller than 2%. For the measurements of the axial repeat of decorated microtubules they are estimated to be less than 0.001 nm^{-1}.

Theoretical solution scattering profiles of kinesin constructs were determined by calculating their Fourier transform, *F*, and then averaging $I = |F|^2$ over all orientations. *F* was calculated from the atomic coordinates by using XPLOR. To this end, the atomic model was put into a large, cubic unit cell in order to obtain a fine sampling of the reciprocal space. Orientational averaging was performed in polar coordinates using bilinear interpolation for calculation of function values in-between the grid points. Calculations were repeated with varying dimensions of the unit cell (up to 10,000 Å) in order to size the effect of discretization errors. As another test, the radius of gyration was determined from the central slope of log *I* vs. s^2 (Guinier plots) for all theoretical scattering curves, and compared with corresponding values calculated directly from the atomic coordinates with XPLOR.

Theoretical solution scattering functions of microtubules and kinesin-decorated microtubules were determined by calculating the azimuthal average of $|F|^2$ of appropriate model structures, corresponding to fiber diffraction intensities with the microtubule axis as fiber axis, followed by orientational averaging over the polar angle according to the assumed uniaxial orientation distribution (for oriented samples; isotropic averaging for true solution scattering). The models were composed of cylindrical elements in order to facilitate the calculation. Bessel functions J_n up to the order $n = 52$ were used to expand the fiber diffraction function.

Results

a) Crystal structures of monomeric and dimeric kinesin constructs

Two constructs from rat kinesin including the N-terminal head domain (amino acids 2-334) and part of the neck region between head and stalk have recently been crystallized and studied by X-ray crystallography (Kozielski et al. 1997 a, b; Sack et al. 1997). The structure described by Sack et al. (1997), based on construct rK354 (amino acids 2–354), is very similar to the structure of the human kinesin construct hK349 determined by Kull et al. (1996). In addition to the Kull structure, it contains the N-terminus and most of the C-terminus (up to residue 351). The second construct, rK379 (amino acids 2-379), includes a considerably longer part of the neck region which was visible up to residue 370 (Kozielski et al. 1997 a). The crystal structure revealed two rK379 molecules interacting with their neck regions by forming an α-helical coiled-coil.

While the short constructs were resolved to about 2 Å, the rK379 could be refined to only 3.0 Å resolution. To gain more confidence in the correctness of the rK379 model, we re-examined the structure by the method of molecular replacement, using an independent native data set and starting with the more reliable structure of the rK354 construct. The new model confirmed the structure of the previous work. Only small differences in the main chain conformation, mainly in the surface loops, were detectable. Larger differences in side chain conformations occur in regions that are not well defined in both structures. The significance of these deviations has yet to be determined. The coiled-coil structure formed by the neck regions of two rK379 molecules is somewhat more symmetric in the new model, presumably due to the slightly better resolution of the new data set (data up to 2.8 Å were used in the refinement). Quantitative measures cited below are based on the new coordinates.

The crystal structure of rK379 is shown in Fig. 1. Crystals of the construct rK379 (amino acids 2-379) are built from pairs of polypeptide chains that form dimers by coiled-coil interaction with their α-helical neck domains (Kozielski et al. 1997 a). The two chains, A and B, of such a dimer are not related by crystallographic symmetry. The rK379 crystals contain two chains – i.e. one dimer – per asymmetric unit.

Crystals of the shorter construct rK354 (amino acids 2-354) contain only one molecule per asymmetric unit (Sack et al. 1997). Although the rK354 molecule has an α-helix at its C-terminal neck domain (as is the case for rK379), there is no obvious interaction between the molecules (besides the crystal contacts) that would justify the grouping of molecules into dimers or higher oligomers. Obviously, the neck helix of the rK354 construct is too short for dimerization by coiled-coil formation. In the following we refer to rK354 crystals as "monomer crystals" and to rK379 crystals as "dimer crystals".

The structure of the kinesin head domain has been described in detail by Kull et al. (1996) and Sack et al. (1997). Here, we adopt the nomenclature used by Sack et al., which is an extension of that introduced formerly (Kull et al.). The kinesin head is a globular, arrow-head shaped domain with a central β-sheet sandwiched between three major α-helices on both sides and framed by two small lobes (β1 a, b, c at one end of the central β-sheet and β5, β5 a, b at the opposite end). The N-terminus is close to the tip of the arrow-head and forms a two-stranded antiparallel β-sheet with a region near the C-terminus of the head (β0 and β9 in the extended nomenclature). The C-terminal region, not visible in the Kull structure, forms another β-strand (β10) that interacts with the core β-sheet at the very tip of the head and finally forms an α-helix (α7) that projects from the tip of the arrow-head in a direction more or less parallel to the "plane" of the core β-sheet.

The general description given above applies to the rK354 monomer and, with small variations, to both heads of the rK379 dimer; only the orientations of the neck helices relative to the head domain vary to a certain extent, as described in more detail below. Figure 1 represents a dimer in an orientation in which head A is very close to the "front view" used as a reference for the monomer structure by Sack et al. (see Figs. 2 a, b in Sack et al. 1997): central β-sheet roughly face-on, tip to the bottom, and neck helix in-plane to the left.

When comparing the kinesin structures as determined from the monomer and the dimer crystals, one has to consider three structures, the monomer and the two molecules of a dimer. There are only small differences in the head domains (amino acids 2-333), as shown by superposition of the monomer and the dimer heads (see Kozielski et al. 1997 a, Fig. 3 a). Since the resolution of the monomer structure is about 2 Å and that of the dimer structure only 3 Å, we will not discuss these differences at the moment. Instead, we will focus on the overall conformations of the kinesin constructs in terms of position and orientation of the neck helices relative to the head domains. At this level of description it is convenient to consider the three structures as composed of two "rigid bodies", the head (amino acids 2-333) and the neck (amino acids 339-351 for the monomer, amino acids 339-370 for the dimer), both connected by a flexible link (amino acids 334-338).

Thus, in the dimer crystals there are two non-crystallographic symmetry operations, one of them transforming the head of molecule A into the head of molecule B, the other one transforming the neck of molecule A into the

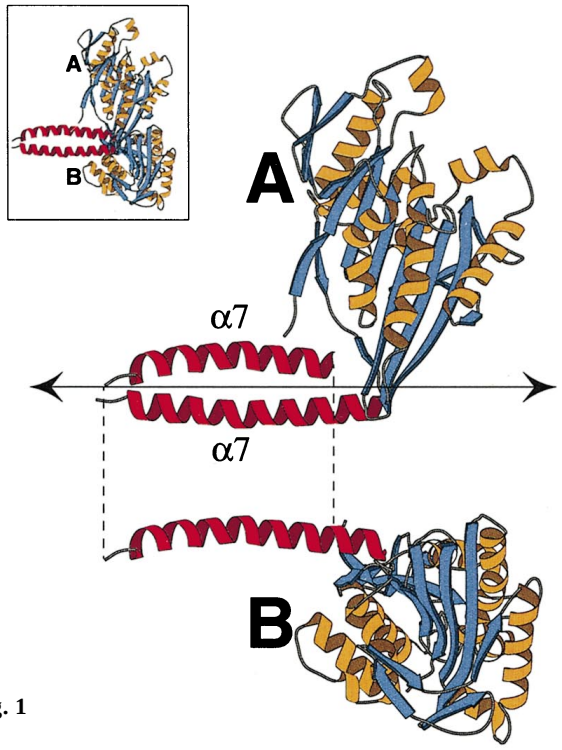

Fig. 1

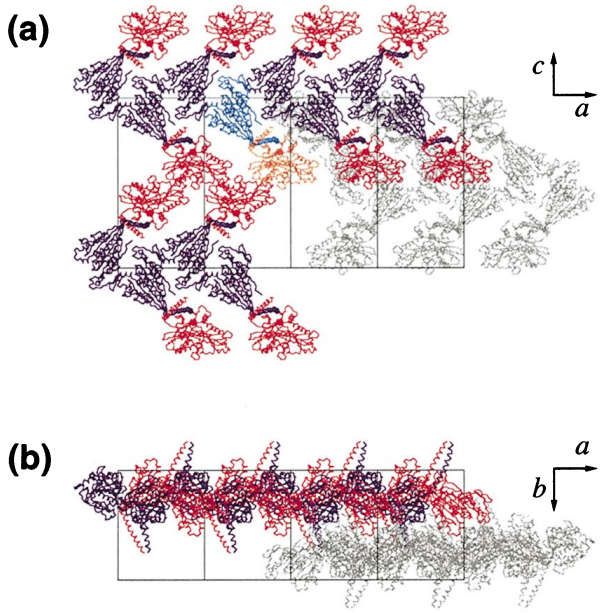

Fig. 2

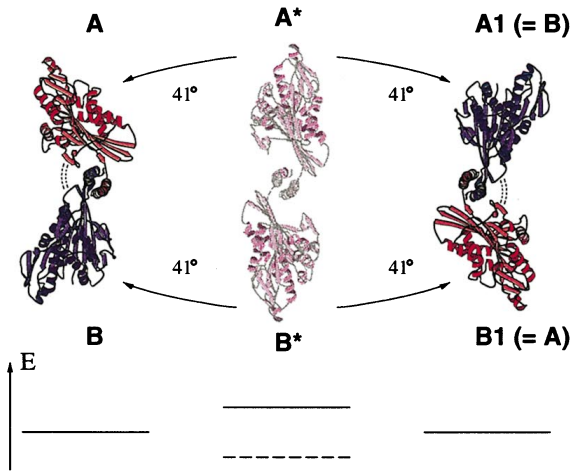

Fig. 3

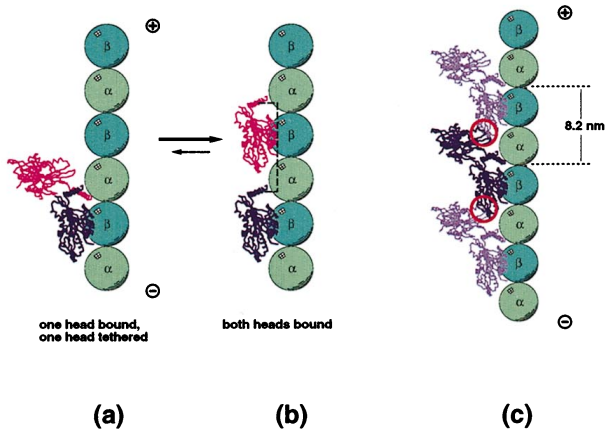

Fig. 7

neck of molecule B. The latter is an almost pure rotation of 180°. (Least squares superposition of the two neck helices by LSQMAN (Kleywegt 1996) yields a rotation angle of 179.8° followed by a translation parallel to the rotation axis of 0.20 Å). It describes the relationship of the two helices of a symmetric coiled-coil. The rotation axis will be called the "neck axis" (horizontal line in Fig. 1).

Heads A and B of a dimer are transformed into each other by a rotation of 117.8° combined with a translation of 1.45 Å along the rotation axis (values determined by least squares superposition of C_α atoms of residues 10-230 and 260-333). This nearly 120° symmetry of the heads is puzzling as it is difficult to imagine how both heads could interact simultaneously with a microtubule – as suggested by "hand-over-hand" models and by decoration experiments – without major conformational changes (Kozielski et al. 1997a; Thormählen et al. 1998a). The natural conclusion from these considerations is that the kinesin dimer dissociates, at least partly, upon interaction with microtubules. In this context an important question is: does the conformation in the crystal reflect intrinsic properties of the kinesin constructs or is it the result of crystal packing?

The molecular arrangements in the monomer and the dimer crystals are entirely different. In the monomer crystal the molecules are rather closely packed with the protrusion of one molecule (α3-loop9-α3a) fitting into a hole near the head-neck junction of another molecule (see Fig. 7 of Sack et al. 1997). The solvent content of the monomer crystals is 49.6% (or 0.985 times the volume of the protein content). The dimer packing can be most eas-

Fig. 1 Structure of the rK379 dimer in the crystalline state. Head A is shown in "front view" (reference orientation used in Sack et al. 1997), head B is shown in a form similar to an "exploded diagram": the head domain is cut from the neck helix and shifted downwards (*dotted lines*) in order to avoid head A being concealed behind head B. The intact dimer is shown by the inset. Figure created using MOLSCRIPT (Kraulis 1991)

Fig. 2 a, b Crystal packing of the dimer crystal (rK379). **a**: One layer of molecules parallel to unit cell axes *a* and *c* shown in red and blue (chains A and B of the dimers; a single dimer is shown in *orange* and *cyan* in order to help distinguishing individual dimers) and a second layer underneath, shown in *gray*. Both layers are related by a twofold screw-axis parallel to *b* (perpendicular to the plane). **b**: View parallel to the layers (same as on top, after 90° rotation about the horizontal). The neck helical coiled coils point off the layers. Figure created using MOLSCRIPT (Kraulis 1991)

Fig. 3 Two conformations of the rK379 dimer in the crystal. The diagram on the left side represents a dimer of rK379 as determined by crystallography in an orientation with the coiled-coil of the neck helices pointing up, perpendicular to the plane of the figure. The diagram on the right side is the same but rotated about 180° around the neck axis. The upper head (A) in the left diagram corresponds to the lower head in the diagram on the right. Because of the symmetry of the coiled-coil, the neck region appears essentially unchanged. The *dashed lines* connecting head A and head B indicate a possible interaction between the heads, for instance by side chain contacts. Instead of considering both diagrams as representations of one conformation of a dimer in two different orientations, they can also be interpreted as showing two different conformations. This is possible because the roles of the two peptide chains are interchangeable. In that case, head A in the left diagram corresponds to head A1 on the right side. The transition between the conformations involves a rotation of 82° of both heads. The center diagram shows a hypothetical conformation (A*B*) derived from the crystal conformation by applying to the heads half the rotation-translation operations required for the transition from the left to the right conformation. The hypothetical conformation has full two-fold symmetry. The free energy is symmetric relative to A*B* and can most likely by represented by a double-well potential. The relationship between the energies of the three conformations is shown below (energy levels in *solid lines*). If the energy of the symmetric state is lower than the energy of the asymmetric states (*dashed line*) the conformation in solution will be symmetric. Figure created using MOLSCRIPT (Kraulis 1991)

Fig. 7 a–c Binding of kinesin dimers to microtubules. Microtubules are represented schematically by tubulin subunits of a single protofilament, with the outer surface of the microtubule assumed to face to the left (tangential view with outside of the microtubule to the left). **a** and **b**: Equilibrium between two binding modes of dimeric kinesin. Part (**a**) shows the dimer after the first step of binding from the solute state. Only one head (purple) is bound to β-tubulin, the conformation is assumed to be the same as in solution and in the crystalline state. The orientation is chosen in such a way that the bound head fits the density deduced by 3D electron microscopy reconstruction of decorated microtubules (Hoenger et al. 1998). Regions α4-loop12 and loop11, which are thought to be responsible for microtubule binding, are oriented towards the free surface area of the protofilament. Part (**b**) shows the dimer after dissociation of the tethered head (magenta) from its counterpart and binding to the next β-tubulin in the direction of the microtubule plus-end. The *dashed line* indicates that both heads could still be connected by more distant parts of their neck or stalk. **c**: Hypothetical arrangement of several dimers to adjacent β-tubulins in the "one head bound – one head tethered" mode. Some parts (*encircled*) of heads belonging to neighboring dimers are interpenetrating. Hence, this arrangement would be forbidden because of steric hindrance or would require accommodation by movement of the tethered head relative to the bound head. Figure created using MOLSCRIPT (Kraulis 1991)

ily imagined as a layered structure with the heads packed in planes parallel to the crystallographic *a* and *c* axes, and the neck helices sticking up and down towards the adjacent layers (Fig. 2). This arrangement creates large holes that could almost accommodate an additional (third) head per dimer. Accordingly, the solvent content of the dimer crystals is considerably higher than that of the monomer crystals (55.6% or 1.25 times the protein content).

Considering the gross differences in crystal packing, the conformation of the kinesin constructs appears to be rather robust. The head conformation up to β10 (preceding the head-neck junction) is virtually identical in both structures. Thus, the location of the neck helix (i.e. the point of attachment to the head) seems to be characteristic for kinesin's structure. To some degree this holds also for the orientation of the neck helix, though this is obviously more variable as can be seen from the variations between the chains A and B of the dimer and the monomer. On the other side, it cannot be excluded that crystal packing affects the orientation of the neck to a certain extent.

Though the rK379 crystal contains only one dimer per asymmetric unit, it actually reveals two different conformations of a dimer. Figure 3, left side, shows the dimer in a view along the neck axis. On the right side, the same is shown after rotation of 180° about the neck axis. The neck coiled-coil appears to be unchanged, since it has two-fold internal symmetry. By contrast, the dimer as a whole has no internal symmetry. In the projections of Fig. 3, the dimer resembles an asymmetric, pointed bracket opened to the left in the original position (left side), and to the right after 180° rotation (right side). Actually, chains A and B of a dimer are non-equivalent in the crystal as the spatial relation between head and neck of chain A is different from that of chain B. However, from a chemical point of view both chains are indistinguishable and therefore, they are potentially equivalent. Thus, by interchanging the roles of A and B, the right side of Fig. 3 can be interpreted in a different way: it also represents another possible conformation of the dimer AB, which is obtained by flipping the head of chain A into position A1, and the head of chain B into position B1.

The transformation from A to A1 (and similarly, from B to B1) is a screw rotation of 81.9° with a translational component of 2.8 Å (least squares superposition of the head C_α atoms). To help picture this, the center of Fig. 3 shows a hypothetical intermediate conformation of the dimer. Positions A* and B* of the hypothetical intermediate are calculated by applying only half the rotation and translation to the original positions A and B. The resulting intermediate state has two-fold symmetry. One could imagine that starting with this hypothetical state, both heads have to be pushed either two the left or to the right in order to obtain one of the two real conformations.

b) Small angle scattering of kinesin in solution

Small angle X-ray scattering (SAXS) can be used to determine gross conformational properties of protein molecules in solution. We have done preliminary SAXS experi-

ments with a resolution of about 5 nm on solutions of monomeric and dimeric kinesin that allow us to compare the solute and the crystal state at the level of the "rigid body" relationship of heads and necks discussed in the previous section.

Solution scattering of two kinesin fragments, rK379 (from rat) and sK338 (from squid), has been measured at concentrations between 5 and 20 mg/ml (Fig. 4, dotted curves, only the 10 mg/ml curves are shown). The sK338 construct from squid kinesin is comparable in size to the rK354 construct that forms monomer crystals. Since the sK338 construct lacks the sequence corresponding to the neck helix $\alpha 7$ in rK354 and rK379, dimerization via coiled-coil formation as in the case of the longer construct rK379 is very unlikely. Accordingly, the radius of gyration determined from the initial slope of the measured curve in Fig. 4 (R_g = 2.20±0.05 nm) is in good agreement with the value calculated for a single molecule of rK354 from the atomic coordinates determined by X-ray crystallography (R_{gc} = 2.09 nm). The measured size is slightly larger than the size calculated from the positions of the atoms. This is presumably due to a contribution of the hydration shell which usually increases R_{gc} by 0.1 to 0.2 nm (cf. Svergun et al. 1998).

The radius of gyration of the rK379 construct is considerably larger than that of the monomeric construct. Extrapolation to zero concentration yields R_g = 4.0±0.2 nm, which is close to the value of R_{gc} = 3.61 nm calculated from the atomic coordinates of a dimer. However, even with the effect of the hydration shell taken into account, the radius of gyration in solution is slightly larger than the value predicted from the crystal structure. Thus, it seems that the center-of-mass distance between the dimer heads could be greater in solution by about 1 nm compared to the crystal conformation (6.1 nm). With our preliminary measurements it would be too early to conclude that the conformations of the rK379 dimer in solution and in the crystal are different in terms of the relative position and orientation of the heads and necks. However, it can be excluded that the dimer adopts an "unfolded" conformation in solution with both heads separated by 8.2 nm (center-of-mass distance) corresponding to the axial repeat of tubulin dimers in microtubules. This is demonstrated by the bottom curve in Fig. 4 which shows the expected scattering of a dimer with the centre-of-mass distance between the heads increased to 8.1 nm by unwinding part of the coiled-coil (up to residue 354, corresponding to "segment I" of Thormählen et al. 1998b). Extension of the range of measurements will be necessary to allow a more detailed analysis of kinesins's structure in solution.

Thus, solution scattering of the kinesin constructs shows at least that the longer construct rK379, which is dimeric in the crystalline state, is also predominantly dimeric in solution. The concentration of rK379 monomers and higher aggregates is negligible compared to the concentration of dimers at total kinesin concentrations of the order of 10 mg/ml. Furthermore, our present small angle scattering data suggest that the distance between the heads of a dimer is somewhat larger in solution compared to the crystalline state.

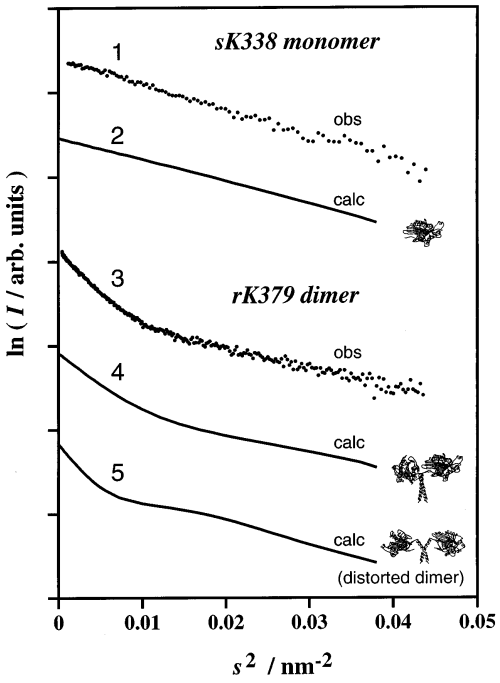

Fig. 4 Small angle X-ray scattering of monomeric and dimeric kinesin fragments in solution. *I* intensity in arbitrary units, $s = 2 \sin \theta/\lambda$, 2θ scattering angle, λ wavelength. *1, 3*: Experimental results obtained with the monomeric construct sK338 (amino acids 2–338 of squid kinesin; *curve 1*) and the dimeric construct rK379 (amino acids 2–379 of rat kinesin; *curve 2*) measured at a protein concentration of 10 mg/ml. *2, 4, 5*: Theoretical scattering intensities calculated from the crystal structures of monomeric and dimeric constructs rK354 (*curve 2*) and rK379 (*curves 4* and *5*). *Curve 5* was calculated for an artificial dimer with the neck region partially unwound to span the distance between adjacent kinesin binding sites on the microtubule surface

c) Small angle scattering of microtubules decorated with kinesin

The interaction of kinesin constructs with microtubules was analyzed by small angle X-ray scattering of microtubules in the presence of kinesin at saturating concentrations. The results are in accord with binding studies and with results from electron microscopy of kinesin-decorated microtubules (Song and Mandelkow 1993; Thormählen et al. 1998a) showing that kinesin binds to β-tubulin with a stoichiometry of one kinesin head per tubulin heterodimer, irrespective of whether the kinesin is monomeric or dimeric in solution.

Figure 5a represents small angle scattering patterns obtained from plain microtubules and microtubules decorated with sK395, a dimeric construct of squid kinesin. Results of model calculations for comparison with the experimental curves of Fig. 5a are presented in Fig. 5b. The main maximum at about 0.05 nm^{-1} is typical for microtubules and corresponds to the first non-zero maximum of the J_0 term in the helical diffraction pattern of microtubules (Mandelkow et al. 1977). The position of this maximum depends on the overall diameter of the microtubules. Thus the peak shift from 0.055 nm^{-1} for plain microtubules to

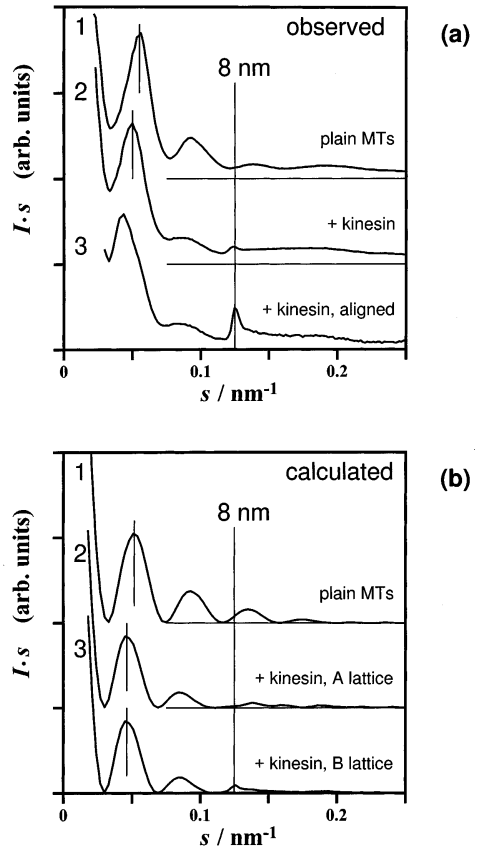

Fig. 5a, b Small angle scattering of kinesin-decorated microtubules in solution. **a**: Experimental results. *1* undecorated microtubules, *2* microtubules decorated with dimeric kinesin construct sK395, *3* oriented gel of sK498-decorated microtubules. Alignment of the microtubules in the oriented gel leads to a shift in position and a change of the shape of the maxima below 0.1 nm^{-1} due to orientation and interference effects. Thus, the central region of the *bottom curve* is not to be compared to the other curves. **b**: Results of model calculations. *1* undecorated microtubule modeled by a hollow cylinder of inner radius 9.5 nm and outer radius 14.0 nm; *2, 3* decorated microtubules modeled by a central hollow cylinder (for the microtubule) and hollow-cylindrical segments fitted to the surface of the central cylinder (for the kinesin molecules). The size of the kinesin segments used for the curves displayed is 4.0 nm in axial direction and 3.03 nm in radial direction with an angular extent of $2\pi/13$ (width). With these dimensions, the volume of the cylinder segments corresponds to one kinesin molecule (sK395) if compared to the volume of a tubulin molecule. The kinesin segments are arranged across the microtubule surface according to the A- or B-lattice, assuming a 13 protofilament microtubule with axial repeat of 8.2 nm and one kinesin molecule per tubulin dimer

0.050 nm^{-1} for decorated microtubules indicates an increase in the mean diameter by about 10%. The second maximum at about 0.9 nm^{-1} in the scattering of undecorated microtubules is strongly reduced in intensity by decoration with kinesin. This is another consequence of the overall increase of the diameter because the intensity ratio of the first and the second peak maximum is a function of the wall thickness.

The shallow maxima at $s \approx 0.13$ nm^{-1} and $s \approx 0.19$ nm^{-1} in the scattering curve of non-decorated microtubules are replaced in the curve of sK395-decorated microtubules by a plateau-like region starting with an accentuated edge at 0.124 nm^{-1} and extending to about 0.2 nm^{-1}. The small intensity peak at $s \approx 1/(8\text{ nm})$ corresponds to the $J_{-3/2}$ spot in the optical diffraction images and is a consequence of the ≈ 8 nm axial periodicity of kinesin decoration.

Theoretical scattering profiles have been calculated for simple model structures representing microtubules as hollow cylinders and bound kinesin molecules as hollow-cylindrical segments tightly attached to the microtubule cylinder. Inner and outer radius of the microtubule cylinder were chosen for optimal fit of calculated and measured scattering profiles of plain microtubules (curves 1 in Figs. 5a and 5b). The position of the kinesin segments on the surface of the microtubule corresponds either to the A- or to the B-surface lattice (curves 2 and 3 in Figs. 5b; Amos and Klug 1974; Mandelkow et al. 1995). The A-lattice is characterized by alternating α- and β-tubulin subunits along the 3-start helices, resulting in a helically symmetric microtubule (13 protofilaments assumed). In the case of the B-lattice, tubulin subunits of the same type follow each other along a 3-start helix, with a discontinuity after each turn where the type of the tubulin subunits changes. Because of this discontinuity, the helical symmetry of the B-lattice microtubules is broken. The outer radius of the cylindrical segments representing kinesin were adjusted to the estimated volume of the molecule at a given axial and angular size of the kinesin segments. Calculations were performed for various combinations of axial and angular extents, but the best results in terms of similarity to the measured profiles were obtained with an axial extent of about 4 nm, corresponding to the height of a tubulin subunit.

In Fig. 5b, model curves 2 (A-lattice) and 3 (B-lattice) are virtually identical at $s < 0.11$ nm^{-1}. However, in the range above 0.11 nm^{-1} the calculations for A- and B-lattice give quite different results. In this range, only the B-lattice calculations are in agreement with the measurements, demonstrating that the overwhelming majority of microtubules in our preparations must be of the B-lattice type in agreement with results from electron microscopy (Song and Mandelkow 1993). The main differences between decorated and non-decorated microtubules can also be found in the calculated scattering profiles. (i) Due to the increase in mean diameter, the main maximum for decorated microtubules is shifted to lower *s*-values compared with non-decorated microtubules. The magnitude of this effect indicates a stoichiometry of one kinesin head per tubulin dimer. (ii) The second maximum (at ≈0.9 nm^{-1}) is reduced in intensity relative to the main maximum. (iii) The B-lattice curve (curve 3) has a distinct peak with maximum at 0.125 nm^{-1} and adjacent to this peak a plateau-like region extending up to ≈0.2 nm^{-1}, in excellent agreement with the experimental results.

The plateau scattering results in part from orientational disorder of the microtubules. The scattering at 1/(8 nm) originates only from those microtubules that are nearly perpendicular to the incident beam. According to the B-lattice, the kinesin molecules are arranged in helical rows with a 10° inclination to the axis. The position of the "8 nm peak" corresponds to the inverse distance between adja-

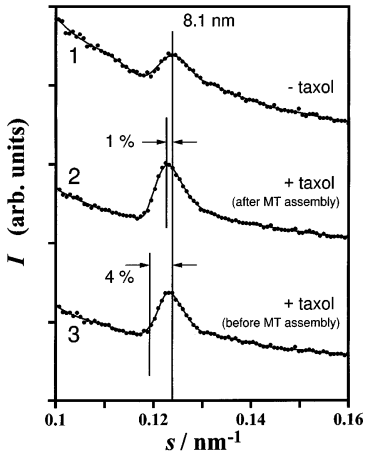

Fig. 6 Effect of taxol on the axial repeat of microtubules probed by small angle scattering of kinesin-decorated microtubules. Microtubules prepared either in the absence of taxol (*1*) or with taxol added after polymerization (*2*) or prior to polymerization (*3*) were decorated with the monomeric kinesin construct sK338. The decorated microtubules were pelleted by centrifugation and partially oriented by uniaxial deformation of the pellet in order to increase the intensity of the peak at $s \approx 0.125$ nm^{-1}. The long vertical line at $s = 0.1237$ nm^{-1} marks the position of the peak in the control curve without taxol. A small shift of maximally 1% may occur if taxol is added prior to polymerization. The *vertical line* at 0.119 nm^{-1} (corresponding to a shift of 4%) indicates where the peak should be expected according to Arnal and Wade (1995) if taxol is added before polymerization. According to small angle scattering the change is definitely not larger than 1% in this case, probably even less

cent rows. Hence, the relation between peak position, s, and true axial repeat, a, is given by $s = 1/(a \cos 10°)$. The correction is only 1.5%, comparable to the absolute accuracy of s values (<2%). With $s = 0.124$ nm^{-1} (see Fig. 5a) the axial repeat turns out to be 8.19 nm ± 0.16 nm. Electron microscopy of negatively stained microtubules generally yields a value of $a = 8.0$ nm. According to Murray (1991), microtubules in frozen hydrated specimen are slightly longer (8.2 nm per dimer) than negatively stained microtubules, presumably due to shrinkage of the latter. Hyman et al. (1995) report a value of $a = 8.1$ nm for frozen hydrated microtubules (normal microtubules, with GDP bound to the E-site of β-tubulin). Thus, our small angle scattering experiment is in excellent agreement with the results from electron cryomicroscopy.

The position of the peak corresponding to the 8 nm axial repeat is independent of interference effects resulting from lateral alignment of microtubules. Considering that the precision of our measurements of the axial repeat of kinesin-decorated microtubules is better than one percent, it should be feasible to monitor small differences of a induced by nucleotide analogs at the exchangeable GTP binding site of tubulin or by treatment with taxol (Vale et al. 1994; Hyman et al. 1995; Arnal and Wade 1995). The sensitivity of the small angle scattering method can even be increased: instead of solutions of decorated microtubules we used gels of densely packed microtubules (obtained by centrifugation) and established a preferential orientation of the microtubules by about tenfold uniaxial extension of the pellet. Both the high concentration and the orientation of the microtubules contribute to a considerable increase in the intensity of the "8 nm peak", while leaving the position of the peak unchanged. Figure 6 shows the result of such measurements with decorated microtubules prepared without taxol (curve 1) or in the presence of taxol (curve 2: taxol added after polymerization; curve 3: taxol added before polymerization). Only the region around 0.125 nm^{-1} is shown. The central part of the scattering function is strongly distorted due to orientation and interference effects, but these effects do not affect the position of the peak under consideration.

According to Vale et al. (1994) the axial repeat of microtubules increases by about 3% when microtubules are polymerized in the presence of taxol ($a = 8.15$ nm without taxol, 8.4 nm with taxol). Arnal and Wade (1995) report a change of almost 4% when microtubules polymerize with taxol; if taxol is added only after polymerization of microtubules, the increase in a is no more than one percent compared to microtubules without taxol. Our measurements using decorated microtubules do not confirm the large changes, but a one percent effect of taxol after polymerization could be possible.

Discussion

a) Kinesin's crystal structure is similar to its structure in solution

The crystal structure of rK379 reveals an asymmetric dimer composed of two potentially equivalent peptide chains that are in non-equivalent conformations. The main forces that are responsible for dimerization stem from symmetric α-helical coiled-coil interactions of the neck helices so that one could expect that the dimer adopts a twofold rotational symmetry. However, the heads deviate from this symmetry and are related to each other by a rotation of almost 120°. To understand kinesin's function in concert with microtubules it is important to know how much the crystal structure is defined by intrinsic properties of the kinesin molecule and how much it results from crystal packing. There are several reasons to assume that the crystal structure of the kinesin dimer, rather than being an artifact, is very similar to its structure in solution.

The first reason is that the conformations of the kinesin molecules in monomer and dimer crystals (rK354 and rK379) are essentially the same; the only difference being the neck helix α7 that points in somewhat different directions in the rK354 monomer and in both chains of the rK379 dimer. Since intermolecular contacts in the monomer and dimer crystals are totally different, it is unlikely that both types of crystal packing result in almost identical refolding of an intrinsically different structure.

This argument implies that at least up to residue Asn334, where significant differences arise first, the crystal structures (virtually identical for rK354 and rK379) reflect a

natural state. This means that the tip of the head domain (as shown in Fig. 1) is indeed the location where the neck is attached to the head domain. The only feature that can be subject to variations depending on the crystal environment, and this to a rather moderate extent, is the direction of the neck relative to the head.

Another reason to believe that the crystal structures are representative for kinesin's natural conformation in solution is the fact that rK354 which is monomeric in solution is also monomeric in the crystalline state, while rK379 which is dimeric in solution (as demonstrated by solution scattering, for instance) is also dimeric in the crystal. This might seem a trivial argument, but in fact it is not because there is no a priori reason that this should be the case. On the contrary, this is consistent with the physical interactions that induce kinesin molecules to form dimers in solution being also the dominant interactions in the crystalline state.

Small angle scattering of rK379 in solution also supports the assumption that the crystal structure is similar to the solution structure. The radius of gyration as well as the form of the scattering profile calculated from the crystal coordinates are in good agreement with the results of the solution scattering experiments. However, there are small deviations between the predictions from the crystal structure and the results of solution scattering suggesting that the rK379 dimer may adopt a somewhat different conformation in solution, with the head-to-head distance enlarged by about 1 nm compared to the crystal structure.

As has been described in the previous section (see Fig. 3), there are two equivalent, but distinct conformations of a rK379 dimer – formally related by interchanging the roles of chains A and B – that both conform to the crystal structure. Since dimerization is essentially a consequence of the coiled-coil interaction in the neck regions with intrinsic two-fold symmetry, it is natural to assume that the observed dimer conformation derives from a parent symmetric state, at least conceptually. The hypothetical intermediate A*B* shown in the center of Fig. 3 seems not to be stable, since the distance between both heads is rather large compared to the crystal structure. Thus the free energy in state A*B* would be higher than in states AB and A1B1 (assuming that the overall interaction of the heads is attractive). However, when considering the flexibility of the head-neck junction (as indicated by the variances between the monomer and dimer structures) it seems possible that the heads adopt another symmetric conformation with a lower free energy. If the energy of this new, relaxed symmetric state is below the energy of the asymmetric states, the dimer will be symmetric in solution.

If the free energy of the symmetric parent state is a local maximum in configuration space (as indicated by the energy levels at the bottom of Fig. 3, continuous lines), the symmetry will be broken spontaneously, resulting in one of two asymmetric conformations. Under real conditions, a pre-selection of one or the other state due to different nucleotide binding states of the heads is conceivable. With regard to the motility of dimeric kinesin this could mean that switching between the two conformations may be triggered by alternating nucleotide hydrolysis. As we have no information about conformational preferences of different nucleotide binding states, we assume here the case with ADP bound to both heads, so that both chains are really equivalent in principle. (The crystal structure of the dimeric kinesin construct is not clear with respect to equivalence of nucleotide binding of both heads. At the present state of analysis a difference in ADP occupancy and/or conformation between the two heads cannot be excluded.)

In the case of spontaneous symmetry breaking, the crystal structure may be representative for the conformation of dimeric kinesin in solution. Nevertheless, transitions between the two alternative conformations may be possible in solution, depending on the height of the energy barrier. According to the crystal structure there are only a few, if any, specific interactions between the two heads. Thus, it seems that the energy required for transitions between both states is rather low. Then, molecules in intermediate states, as suggested by Fig. 3, might also be present. The resolution of our preliminary small angle scattering measurements would not suffice to discriminate these intermediate states, unless they differed very much in conformation from the limiting states. However, it can be excluded that an appreciable number of dimers are in (transient) states with both heads separated by a distance large enough to bind to adjacent β-tubulins along the protofilament of a microtubule.

From the above considerations the structure of the dimeric kinesin construct rK379 in solution can be pictured as follows: Two molecules dimerize by forming a symmetric coiled-coil of their neck helices α7. The heads are folded very much in the same way as in the crystalline state, up to residue ≈334 (β10). Their shape resembles that of a cone with the tip (close to β10) pointing "downwards", to the neck. There are a few amino acids in-between the tip of the cone and the start of the coiled-coil (residues ≈335 to 338, head-neck junction), which confer some degree of flexibility to the whole structure. In the first instance, the symmetry of the coiled-coil could favor an arrangement of the heads that is also symmetric. This fully symmetric state corresponds to a maximum or a minimum of the free energy. If the free energy is maximal, the symmetry will be broken: rotation of the heads about their respective points of attachment to the neck will minimize the free energy by enabling the heads to interact more closely. This leads to one of two equivalent, non-symmetric conformations. Our preliminary solution scattering results are compatible with the assumption that this conformation is similar, if not identical, to that found in the crystal. However, other conformations resulting from different rotations of the heads (including the symmetric conformation, which has a larger head-to-head distance) also seem possible. In any case, the heads are attached to the neck with their tips in close proximity to each other, thus their radius of action is considerably restricted as long as the neck is unchanged.

b) Implications for the interaction with microtubules

If kinesin's structure in solution is similar to that in the crystalline state, this may have consequences for the bind-

ing to microtubules, for instance in decoration experiments. We do not consider here motility and force generation of a single kinesin dimer as this requires knowledge of the conformational effects stimulated by nucleotide processing. For the present discussion we assume only that both heads of a dimer are potentially equivalent. This should be the case if the same type of nucleotide (e.g. ADP or AMPPNP, a non-hydrolyzable ATP analogue) is bound to both heads.

Because of the nearly 120° relationship between the heads it is evident that a dimer in the solute conformation cannot bind immediately with both heads to a microtubule, at least not in an equivalent way. (There is no 120° symmetry relationship between tubulin dimers of a microtubule.) On the other side, our small angle scattering of decorated microtubules, as well as other experiments (Thormählen et al. 1998a) indicate that both heads bind simultaneously to adjacent β-tubulins. This is not possible without a major conformational change, presumably by partial unwinding of the coiled-coil in the neck region (Kozielski et al. 1997a; Thormählen et al. 1998a). Thus, binding of dimeric kinesin to microtubules appears as a two-step process as illustrated in Fig. 7. In the first step (Fig. 7a) only one head of the kinesin dimer binds to a β-tubulin while the whole dimer retains its solution structure. Thus, the second head is sitting "piggyback" on top of the first without contact to the microtubule. In the second step the heads dissociate, at least partly, in such a way that the second head can bind to the next β-tubulin in very much the same way as the first head (Fig. 7b).

The orientation of the bound heads in Fig. 7 takes into account that secondary structure elements thought to be involved in tubulin binding are facing the microtubule surface (Woehlke et al. 1997). Three-dimensional reconstruction of microtubules decorated with rK379 has been used to determine the orientation of the bound heads by fitting kinesin's crystal structure into the structure of decorated microtubules determined by cryo-electron microscopy (Hoenger et al. 1998). Nevertheless, the orientation of the bound heads is only known with a considerable amount of uncertainty.

As long as the nucleotide states of both heads are unchanged, step two is reversible, at least in principle. Thus, it is conceivable that both types of binding shown in Figs. 7a and 7b can occur simultaneously. Depending on solution conditions, one or the other state might be predominant. Three-dimensional reconstructions of kinesin-decorated microtubules by Hirose et al. (1996) and Arnal et al. (1996) have been interpreted by assuming a binding of one dimer per β-tubulin (corresponding to Fig. 7a). In our hands, on the contrary, decoration of microtubules with dimeric kinesin always results in a situation corresponding to Fig. 7b, i.e. both heads of a dimer bind to adjacent β-tubulins (Thormählen et al. 1998a; Hoenger et al. 1998).

If we consider the transition between both states depicted in Figs. 7a and 7b as a reversible reaction, this means that in our experiments the equilibrium is totally on the right side. In other words, the gain in free energy due to the binding of the second head to the microtubule outweighs by far the free energy needed for separation of the heads of a dimer. The conclusion would be that the interaction between tubulin and kinesin is stronger than the interaction between two kinesin heads. After all, this is not too surprising, as a strong interaction between kinesin and tubulin appears to be a prerequisite for force generation. Our failure to detect the predicted ≈4% taxol effect on the axial repeat of microtubules by using small angle solution scattering of kinesin-decorated microtubules could be interpreted as another indication of a strong interaction between kinesin and tubulin: one way to reconcile our negative results with the findings from electron microscopy (Vale et al. 1994; Arnal and Wade 1995) would be to assume that binding of kinesin to tubulin is strong enough to suppress the conformational effect of taxol on microtubules.

A difference in free energy may explain a preference of the "both-heads-bound state" (Fig. 7b) over the "one-head-bound-one-head-tethered state" (Fig. 7a) at low concentrations of kinesin. However, this is not sufficient to explain the stoichiometry of one head per tubulin dimer that we found at saturating conditions by small angle scattering and other methods (for a detailed account of the question of stoichiometry see Thormählen et al. (1998a)). At saturating concentrations, it would be energetically more favorable to have all β-tubulins occupied by an intact kinesin dimer, rather than a single head. In this way the maximum number of strong tubulo-kinesin interactions would be attained without the expense of free energy required for dissociation of kinesin dimers.

A possible explanation why this seems not to be the case is sketched in Fig. 7c. If we accept that the structure of the kinesin dimer is as deduced from the crystal structure, and if the orientation of the dimer, when bound to a β-tubulin, is as shown in Fig. 7a, then it would be impossible to bind another dimer to a neighboring β-tubulin because of steric hindrance between the two kinesin dimers. Under these circumstances, the energetic argument of the previous paragraph no longer holds true, and the limiting stoichiometry should be one head per tubulin dimer. It should be mentioned that in contrast to kinesin, the retrograde motor ncd appears to bind with a stoichiometry of one dimer per tubulin dimer (Hirose et al. 1996; Sosa et al. 1997; Lockhart et al. 1995; Crevel et al. 1996). This notable difference to kinesin could be explained by assuming that steric hindrance does not occur in the case of ncd. Rather small variances in the conformations of the ncd and the kinesin dimer molecules would be sufficient to account for this difference.

Whether steric hindrance really plays a role in decoration of microtubules with kinesin or not, a lesson to learn from the above is that even seemingly minor details can have unexpectedly large and surprising effects. In this context it is tempting to speculate on the origin of the opposite directionality of kinesin and ncd movement. As already suggested by Hirose et al. (1996), this could be caused by a somewhat different position of the second, tethered head after the first head has bound to β-tubulin. In the case of kinesin, they assume that the second head points to the plus-end, thus biasing the direction of movement, while in the case of ncd the reverse should be true.

This argument conforms completely with the situation illustrated by Fig. 7a. It seems suggestive to assume that the second head in Fig. 7a will prefer binding to the next β-tubulin in plus-end direction once it has dissociated from the other head.

Acknowledgements We thank H. D. Bartunik, G. Bourenkov and A. Popov for help with the MPG/GBF beamline BW6, as well as A. Thompson and V. Biou for help with ESRF beamline BM14. We are also grateful to M. H. J. Koch for making small angle beamline X33 of the EMBL outstation at DESY in Hamburg available and to M. H. J. Koch and D. Svergun for helpful suggestions concerning the interpretation of the solution scattering data. This research was funded by grants from the DFG and BMBF.

References

Amos LA, Klug A (1974) Arrangement of subunits in flagellar microtubules. J Cell Sci 14:523–549

Arnal I, Metoz F, Debonis S, Wade RH (1996) Three-dimensional structure of functional motor proteins on microtubules. Curr Biol 6:1265–1270

Arnal I, Wade RH (1995) How does taxol stabilize microtubules. Curr Biol 5:900–908

Brady ST (1995) A kinesin medley – biochemical and functional heterogeneity. Trends Cell Biol 5:159–164

Brünger AT (1992) X-PLOR version 3.1. A system for X-ray crystallography and NMR. Yale University Press, New Haven, CT, USA

Cambillau C, Roussel A, Inisan AG, Knoops-Mouthuy E (1996) Turbo-Frodo version 5.5, AFMB-IFRC1 chemin. Aiguier, Marseille, France

Cole DG, Scholey JM (1995) Structural variations among the kinesins. Trends Cell Biol 5:259–262

Collaborative Computing Project No. 4 (1994) CCP4 suite of programs. Acta Cryst. D 50, 760–763

Crevel IMTC, Lockhart A, Cross RA (1996) Weak and strong states of kinesin and ncd. J Mol Biol 257:66–76

Cross RA (1997) The natural economy of kinesin. Curr Biol 7:R631–R633

Gilbert SP, Moyer ML, Johnson KA (1998) Alternating site mechanism of the kinesin ATPase. Biochemistry 37:792–799

Hirokawa N (1996) The molecular mechanism of organelle transport along microtubules: the identification and characterization of KIFs (kinesin superfamily proteins). Cell Struct Funct 21:357–367

Hirose K, Lockhart A, Cross RA, Amos LA (1996) Three-dimensional cryoelectron microscopy of dimeric kinesin and ncd motor domains on microtubules. Proc Natl Acad Sci USA 93:9539–9544

Hoenger A, Sack S, Thormählen M, Marx A, Müller J, Gross H, Mandelkow E (1998) Image reconstructions of microtubules decorated with monomeric and dimeric kinesins: comparison with X-ray structure and implications for motility. J Cell Biol 141:419–430

Holmes KC (1997) The swinging lever-arm hypothesis of muscle contraction. Curr Biol 7:R112–R118

Hyman AA, Chretien D, Arnal I, Wade RH (1995) Structural changes accompanying GTP hydrolysis in microtubules: information from a slowly hydrolyzable analogue guanylyl-(α,β)-methylene-diphosphonate. J Cell Biol 128:117–125

Jiang W, Stock MF, Li X, Hackney DD (1997) Influence of the kinesin neck domain on dimerization and ATPase kinetics. J Biol Chem 272:7626–7632

Kleywegt GJ (1996) Use of non-crystallographic symmetry in protein structure refinement. Acta Cryst D 52:842–857

Koch M, Bordas J (1983) X-ray diffraction and scattering on disordered systems using synchrotron radiation. Nucl Instrum Methods 208:461–469

Kozielski F (1997) Die Röntgenstrukturanalyse des Motorproteins Kinesin. Ph.D. thesis, Universität Hamburg, Germany

Kozielski F, Sack S, Marx A, Thormählen M, Schönbrunn E, Biou V, Thompson A, Mandelkow E-M, Mandelkow E (1997a) The crystal structure of dimeric kinesin and implications for microtubule-dependent motility. Cell 91:985–994

Kozielski F, Schönbrunn E, Sack S, Müller J, Brady S, Mandelkow E (1997b) Crystallization and preliminary X-ray analysis of monomeric and dimeric kinesin motor domains. J Struct Biol 119:28–34

Kraulis PJ (1991) Molscript: a program to produce both detailed and schematic plots of protein structures. J Appl Cryst 24:946–950

Kull FJ, Sablin E, Lau P, Fletterick R, Vale R (1996) Crystal structure of the kinesin motor domain reveals a structural similarity to myosin. Nature 380:550–554

Lockhart A, Crevel IMTC, Cross RA (1995) Kinesin and ncd bind through a single head to microtubules and compete for a shared mt binding-site. J Mol Biol 249:763–771

Ma YZ, Taylor EW (1997) Interacting head mechanism of microtubule-kinesin ATPase. J Biol Chem 272:724–730

Mandelkow E, Thomas J, Cohen C (1977) Microtubule structure at low resolution by x-ray diffraction. Proc Natl Acad Sci USA 74:3370–3374

Mandelkow E-M, Herrmann M, Ruehl U (1985) Tubulin domains probed by limited proteolysis and subunit-specific antibodies. J Mol Biol 185:311–327

Mandelkow E, Song Y-H, Mandelkow E-M (1995) The microtubule lattice – dynamic instability of concepts. Trends Cell Biol 5:262–266

Murray JM (1991) Structure of flagellar microtubules. Int Rev Cytol 125:47–93

Murshudov G, Vagin A, Dodson E (1996) In: Dodson E, Moore M, Ralph A, Bailey S (eds) Macromolecular refinement. Proceedings of the CCP4 Study Weekend. SERC Daresbury Laboratory, Warrington, UK, pp 93–104

Navazza J (1994) AMoRe: an automated package for molecular replacement. Acta Cryst A 50:157–163

Otwinowski Z, Minor W (1997) Processing of X-ray diffraction data collected in oscillation mode. Methods Enzymol 276:307–326

Rayment I (1996) Kinesin and myosin: molecular motors with similar engines. Structure 4:501–504

Sablin EP, Kull FJ, Cooke R, Vale RD, Fletterick RJ (1996) Crystal structure of the motor domain of the kinesin-related motor ncd. Nature 380:555–559

Sack S, Müller J, Marx A, Thormählen M, Mandelkow E-M, Brady ST, Mandelkow E (1997) X-ray structure of motor and neck domain from rat brain kinesin. Biochemistry 36:16155–16165

Song Y-H, Mandelkow E (1993) Recombinant kinesin motor domain binds to β-tubulin and decorates microtubules with a B surface lattice. Proc Natl Acad Sci USA 90:1671–1675

Sosa H, Dias DP, Hoenger A, Whittaker M, Wilson-Kubalek E, Sablin E, Fletterick RJ, Vale RD, Milligan RA (1997) A model for the microtubule-ncd motor protein complex obtained by cryoelectron microscopy and image-analysis. Cell 90:217–224

Svergun D, Richard S, Koch MHJ, Sayers Z, Kuprin S, Zaccai G (1998) Protein hydration in solution: Experimental observation by x-ray and neutron scattering. Proc Natl Acad Sci USA 95:2267–2272

Thormählen M, Marx A, Müller SA, Song Y-H, Mandelkow E-M, Aebi U, Mandelkow E (1998a) Interaction of monomeric and dimeric kinesin with microtubules. J Mol Biol 275:795–809

Thormählen M, Marx A, Sack S, Mandelkow E-M (1998b) The coiled-coil helix in the neck of kinesin. J Struct Biol (in press)

Vale RD (1996) Switches, latches, and amplifiers: common themes of G proteins and molecular motors. J Cell Biol 135:291–302

Vale RD, Coppin CM, Malik F, Kull FJ, Milligan RA (1994) Tubulin GTP hydrolysis influences the structure, mechanical properties, and kinesin-driven transport of microtubules. J Biol Chem 269:23769–23775

Vale RD, Fletterick RJ (1997) The design plan of kinesin motors. Annu Rev Cell Dev Biol 13:745–777

Woehlke G, Ruby AK, Hart CL, Ly B, Hom-Booher N, Vale RD (1997) Microtubule interaction site of the kinesin motor. Cell 90:207–216